Knockdown of PGBD5 inhibits the malignant progression of glioma through upregulation of the PPAR pathway

PENGREN LUO[1-3*], JINHONG YANG[3*], LIPENG JIAN[1], JIGEN DONG[1], SHI YIN[1], CHAO LUO[1] and SHUAI ZHOU[1-3]

[1]Department of Neurosurgery, The First People's Hospital of Yunnan Province; [2]Department of Neurosurgery, The Affiliated Hospital of Kunming University of Science and Technology; [3]Medical School, Kunming University of Science and Technology, Kunming, Yunnan 650500, P.R. China

Received November 1, 2023; Accepted February 5, 2024

DOI: 10.3892/ijo.2024.5643

Abstract. Glioma is the most common type of primary intracranial malignant tumor, and because of its high invasiveness and recurrence, its prognosis remains poor. The present study investigated the biological function of piggyBac transportable element derived 5 (PGBD5) in glioma. Glioma and para-cancerous tissues were obtained from five patients. Reverse transcription-quantitative PCR and western blotting were used to detect the expression levels of PGBD5. Transwell assay and flow cytometry were used to evaluate cell migration, invasion, apoptosis and cell cycle distribution. In addition, a nude mouse tumor transplantation model was established to study the downstream pathways of PGBD5 and the molecular mechanism was analyzed using transcriptome sequencing. The mRNA and protein expression levels of PGBD5 were increased in glioma tissues and cells. Notably, knockdown of PGBD5 *in vitro* could inhibit the migration and invasion of glioma cells. In addition, the knockdown of PGBD5 expression promoted apoptosis and caused cell cycle arrest in the G_2/M phase, thus inhibiting cell proliferation. Furthermore, *in vivo* experiments revealed that knockdown of PGBD5 expression could inhibit Ki67 expression and slow tumor growth. Changes in PGBD5 expression were also shown to be closely related to the peroxisome proliferator-activated receptor (PPAR) signaling pathway. In conclusion, interference with PGBD5 could inhibit the malignant progression of glioma through the PPAR pathway, suggesting that PGBD5 may be a potential molecular target of glioma.

Correspondence to: Dr Shuai Zhou, Department of Neurosurgery, The First People's Hospital of Yunnan Province, 157 Jinbi Road, Kunming, Yunnan 650500, P.R. China
E-mail: zshuai@kust.edu.cn

*Contributed equally

Key words: glioma, PGBD5, tumor growth, PPAR signaling, transposons

Introduction

Glioma is the most common type of primary malignant tumor of the central nervous system worldwide. Glioma is associated with high rates of disability and mortality, and a poor prognosis (1). According to the World Health Organization (WHO) pathological classification, grades I and II represent low-grade glioma (LGG), whereas grades III and IV represent high-grade glioma (HGG) (1). Among all glioma cases, glioblastoma (GBM) accounts for ~57% in the US, and its median survival time is <2 years (2). Although the survival duration of patients with LGG is longer than HGG, this type of tumor may eventually progress to HGG after multiple relapses (3,4). At present, the preferred treatment for glioma remains surgical resection with maximum safety, with temozolomide chemotherapy and radiotherapy as auxiliary methods (5). However, owing to characteristics such as drug resistance, radiotherapy resistance and frequent recurrence of glioma, therapeutic efficacy remains poor (6,7). Therefore, identifying effective molecular targets (8-11) that help navigate this issue in glioma treatment is necessary.

Transposons or transposable elements (TEs) are present in almost all organisms; these mobile genetic elements account for ~50% of the human genome (12,13). Transposons are usually classified as RNA-based retrotransposons and 'cut-paste' or 'cut-copy' types of transposons (14). Transposons not only serve an active role in the regulation of gene expression, but can occasionally impose negative effects, as their insertion into genes may disrupt normal gene function and cause genomic instability. They maintain genomic diversity and promote adaptive evolution (15), thus serving as a crucial factor at different stages of human growth and development (16). However, owing to the adverse effects of TE on the genome, they are usually inactive (17) and the expression mode of TE is strictly regulated during the human lifespan (18). Evidence from published studies has shown that changes in the regulatory mechanisms of TE may lead to genomic instability, chromosome breakage and carcinogen activation, triggering the development of various immune, neurological and genetic diseases (19-21).

PiggyBac transposons are a category of TE. At present, five complete piggyBac elements have been identified, namely piggyBac transportable element derived (PGBD)1, 2, 3, 4 and

5 (22). Genomic data have shown that PGBD5 in humans is the most conserved piggyBac sequence. This gene can form a 'cut-paste' type of DNA transposon (23). PGBD5 is synthesized in human cells in response to certain cellular conditions or signals. This includes during developmental stages, in the presence of inflammatory signals, and possibly in response to processes that can lead to cancer. Its DNA transposition must occur in the entire genome for the transposon to be precisely excised and preferentially inserted into TTAA sites (24,25). The expression of PGBD5 in humans and mice has been shown to be primarily limited to some regions of the early embryonic and adult brains (26,27). In mice, PGBD5 is primarily expressed in the nucleus, preferentially in specific areas of the brain and central nervous system, which are rich in granulosa cells; therefore, PGBD5 may be primarily expressed in granulosa cells, which are a small population of neurons different from other nerve cells in terms of morphology and function; some of these cells can exert effects in adult nerve growth (26). Relevant studies have shown that the expression of PGBD5 is sufficient to not only promote carcinogenic genome rearrangement (28,29), but can also induce non-anchored cell growth *in vitro* and tumor formation *in vivo*. Consequently, the transformation of cells induced by PGBD5 has been linked to various chromosomal alterations, including deletions, inversions and translocations (28). In addition, in other studies, abnormal PGBD5 expression has been reported in neural tissues and most solid tumors in children, such as medulloblastoma, rhabdomyoma, neuroblastoma, Ewing's sarcoma and ependymoma (25,26,28). PGBD5 is frequently upregulated in solid tumors in children and adults, suggesting its role in cancer development through inducing DNA rearrangements. This upregulated pattern offers a plausible mechanism for site-specific genomic alterations observed in carcinogenesis (28). In a recent study, a survival-risk prediction model was established using bioinformatics methods. According to the model, the expression of PGBD5 was negatively associated with the survival period of GBM, and it served as a marker of poor prognosis (30).

Peroxisome proliferator-activated receptors (PPARs) are ligand-induced transcription factors that belong to the nuclear receptor family (31). When integrating with ligands, PPARs translocate to the nucleus, bind to peroxisome promoter response elements on DNA and heterodimerize with retinoic-acid X receptor. When a ligand binds to a PPAR, it primarily acts as a transcriptional regulator of specific target genes (32). The role of PPARs in lipid glucose metabolism and the regulation of homeostasis has been studied widely. In mammals (33), three subtypes of PPAR are present: PPARα, PPARβ/δ and PPARγ, and their biological distribution patterns and ligand affinity vary widely in different organs (34). PPARα is primarily expressed in the liver, heart, kidney, intestine, brown fat and skeletal muscle, activating fatty acid catabolism and gluconeogenesis to regulate energy balance. In the past decade, increasing evidence has shown that PPARα can regulate one or more pathways to adjust tumorigenesis (35). However, contradictory effects of PPARα on tumor regulation have been identified. Relevant studies have shown that a reduction in the transcriptional activity of PPARα enhances cell migration and invasion *in vitro* (36,37), and PPARα agonists can restore normal cellular behavior in cancer cell lines (38). Another study demonstrated that PPARα upregulation activates liver cancer stem cells and promotes the occurrence of early hepatocellular carcinoma (39). PPARβ/δ are commonly expressed in various tissues; however, their biological functions vary within these tissues. In addition, the roles of PPARβ/δ in various cancer cell models differ and remain unclear (40). PPARγ has two subtypes: PPARγ1 and PPARγ2; the former is dominant and is commonly expressed in various tissues, whereas the latter is primarily confined to adipose tissues. The primary functions of PPARγ include regulation of the glucose-lipid balance, insulin sensitivity, adipogenesis, inflammation, immune response and tumorigenesis (41).

Prior studies have indicated that PGBD5 is not only involved in the regulation of gene expression, but is associated with genomic instability and chromosome rearrangements. Therefore, the present study aimed to investigate PGBD5 in glioma. Existing research has suggested that PGBD5 is highly expressed in various solid tumors, including glioma, in both children and adults (28). This provides a strong foundation for exploring its relevance in glioma pathogenesis. The present study aimed to assess the specific molecular functions and roles of PGBD5 in glioma, to understand whether its silencing inhibits the proliferation, migration and invasion of glioma cells. The present study explored the molecular mechanisms contributing to glioma formation, with the aim of improving understanding.

Materials and methods

Tissues. A total of five patients (age range, 36-64 years; mean age, 48.6 years) with glioma were recruited from the Department of Neurosurgery, The First People's Hospital of Yunnan Province (Kunming, China) between October and December 2021. The exclusion criteria included patients with a history of neurological disorders other than glioma, those who had undergone chemotherapy or radiation therapy within the last 6 months, and individuals <18 or >65 years old. Paired tumor tissues and para-cancerous tissues, located at a specified distance of 2 cm from the tumor margin, were obtained from the same patients. Only patients from whom para-cancerous tissues could be successfully harvested during surgical resection were included in the study. Tissues were collected at the time of tumor resection to ensure the relevance and freshness of the samples for subsequent analysis. Among the five patients, three were male and two were female. Preoperative diagnosis ruled out other tumors and chronic diseases, and the patients were yet to undergo any treatment for glioma. The tumor pathological grades corresponding to the tested specimens were as follows Two cases of anaplastic astrocytoma (WHO III) and three cases of GBM (WHO IV). The tissues obtained from each patient underwent immunohistochemistry analysis to detect specific proteins, including GFAP and IDH1. The staining intensity was evaluated by at least two professional pathologists (data not shown). Residual tumor tissues and adjacent tissues were collected after pathological examination and were immediately stored in liquid nitrogen. After the immunohistochemical diagnosis was confirmed, the tissues were used for further research. The enrolled patients provided written informed consent, the experimental contents complied with relevant national regulations, and the experimental procedures

Table I. List of primers and shRNA sequences used.

Name	Sequence
PGBD5-F	5'-CATGTCCTTGATCTGCTGGTAC-3'
PGBD5-R	5'-TGATGGCGAACCAGAACACCTG-3'
β-actin-F	5'-CCTTCCTGGGCATGGAGTC-3'
β-actin-R	5'-TGATCTTCATTGTGCTGGGTG-3'
sh-PGBD5 #1	5'-GCAGAUACGAUGACAAAUATTCTCGAGUAUUUGUCAUCGUAUCUGCTT-3'
sh-NT	5'-CCTAAGGTTAAGTCGCCCTCGCTCGAGCGAGGGCGACTTAACCTTAGG-3'

Underlining indicates the hairpin structure of shRNA. F, forward; PGBD5, piggyBac transportable element derived 5; PPAR, peroxisome proliferator-activated receptor; R, reverse; sh, short hairpin.

were approved by the Ethics Committee of the Medical School at Kunming University of Technology (approval no. KMUST-MEC-092; Kunming, China). The study was conducted in accordance with The Declaration of Helsinki.

Cell culture. Human glioma cell lines [A172, U251 and U87 MG (American Type Culture Collection version, GBM cell line of unknown origin, hereinafter referred to as U87)] and normal human astrocytes (NHAs; cat. no. CP-H122) were purchased from Procell Life Science & Technology Co., Ltd. The cells were examined using short-tandem repeat profiling to confirm authenticity and to ensure they were free from cross-contamination. A172, U251 and NHA cells were individually cultured in Dulbecco's modified Eagle medium (Biological Industries; Sartorius AG) supplemented with 10% fetal bovine serum (FBS; Gibco; Thermo Fisher Scientific, Inc.) in a 5% CO_2-humidified atmosphere at 37˚C. U87 cells were cultured in minimum essential medium-non-essential amino acids (Biological Industries; Sartorius AG) supplemented with 10% FBS in a 5% CO_2-humidified atmosphere at 37˚C. Penicillin was added to all media at a concentration of 100 U/ml.

Reverse transcription-quantitative PCR (RT-qPCR). Total RNA was isolated from glioma tissues and A172, U251 and U87 cell lines using RNAIso Plus (Takara Biotechnology, Ltd.; cat. no. 9108) and reverse-transcribed to cDNA using a HiScript III All-in-one RT SuperMix Perfect for qPCR kit (Vazyme Biotech Co., Ltd.) according to the manufacturer's protocol. qPCR was performed using a ChamQ Universal SYBR qPCR Master Mix Kit (Vazyme Biotech Co., Ltd.) and a LightCycler480II (Roche Diagnostics), with an initial denaturation step at 95˚C for 5 sec, followed by a joint annealing and extension step at 60˚C for 20 sec. Relative mRNA expression levels were determined using the $2^{-\Delta\Delta Cq}$ method (42), normalized to β-actin and represented graphically using GraphPad Prism 9.0 (Dotmatics). The sequences of primers (TsingKe Biological Technology) are listed in Table I.

Western blotting. Proteins were extracted from glioma tissues or cells using the radioimmunoprecipitation assay lysis buffer (Beijing Solarbio Science & Technology Co., Ltd.) containing a protease inhibitor (Bimake). Proteins were quantified using a bicinchoninic acid kit (Beyotime Institute of Biotechnology) and the final protein system had a concentration of 40 μg/lane. The proteins were then separated by sodium dodecyl sulfate-polyacrylamide gel electrophoresis on 10% gels and transferred to polyvinylidene fluoride membranes (MilliporeSigma). After blocking with 5% skimmed milk for 1.5 h at room temperature, the membranes were incubated with primary antibodies (dilution 1:1,000) overnight at 4˚C. The membranes were then washed three times with TBS-0.1% Tween (TBST) for 10 min at room temperature, after which, they were incubated with goat anti-rabbit IgG (dilution 1:5,000) or anti-mouse IgG (dilution 1:5,000) horseradish peroxidase-conjugated secondary antibodies (both from ABclonal Biotech Co., Ltd.) for 1 h at room temperature. Subsequently, the membranes were washed three times with TBST for 10 min. Finally, exposure and development were performed using a super ECL developer solution (ABP Biosciences, LLC). Blots were detected using the ChemiDoc XRS+ Gel imaging system (Bio-Rad Laboratories, Inc.) and were semi-quantified using Image Lab 6.0.1 (Bio-Rad Laboratories, Inc.). The list of antibodies used in the present study is included in Table II.

Lentivirus production. The GV248 lentiviral vector containing a short hairpin RNA (shRNA) targeting PGBD5 (sh-PGBD5) and the negative control (NC) vector (sh-NC) containing a non-targeting shRNA sequence were established by Shanghai GeneChem Co., Ltd. and were ready to directly infect the cells. The shRNA sequence (and negative control sequence) is provided in Table I and matches the sequence reported in a previous study (29). The element sequence of the vector is hU6-MCS-Ubiquitin-enhanced green fluorescent protein (EGFP)-IRES-puromycin.

Lentivirus infection. A172, U251 and U87 cells ($5x10^4$/well) were evenly spread into 6-well plates for culture. After ~10 h, when the cells completely adhered to the well, the level of cell fusion was controlled at ~30%. The following formula was used to calculate the required viral titer: Virus volume=(MOI x cell count)/virus titer, where MOI refers to multiplicity of infection, and a MOI of 10 was used to infect the cells. Subsequently, the original culture medium was replaced with culture medium containing lentiviruses for further culture. The culture medium was refreshed again after 12 h at 37˚C. Because the EGFP gene sequence is present in lentiviruses, its expression could be observed in all three cell lines 72 h after infection under a fluorescence microscope equipped with appropriate filter sets for GFP detection. In addition, the lentivirus carries a puromycin

Table II. List of antibodies used.

Antibody	Supplier (cat. no.)
PGBD5 Mouse mAb	Thermo Fisher Scientific, Inc. (cat. no. MA5-32886)
β-actin Mouse mAb	ABclonal Biotech Co., Ltd. (cat. no. AC004)
CDK1 Rabbit mAb	ABclonal Biotech Co., Ltd. (cat. no. A11420)
Cyclin B1 Rabbit pAb	ABclonal Biotech Co., Ltd. (cat. no. A16800)
GAPDH Mouse mAb	ABclonal Biotech Co., Ltd. (cat. no. AC002)
HRP Goat Anti-Rabbit IgG	ABclonal Biotech Co., Ltd. (cat. no. AS014)
HRP Goat Anti-Mouse IgG	ABclonal Biotech Co., Ltd. (cat. no. AS003)
Bax Rabbit Antibody	Cell Signaling Technology, Inc. (cat. no. 2772)
Bcl-2 Rabbit mAb	Cell Signaling Technology, Inc. (cat. no. 3498)
Caspase-3 Rabbit Antibody	Cell Signaling Technology, Inc. (cat. no. 14220)
Ki-67 Rabbit Antibody	MXB Biotechnologies (cat. no. RMA-0731)
PPARδ Mouse Antibody	Abmart Pharmaceutical Technology Co., Ltd. (cat. no. MN51264)
p-PPARδ (Thr256) Rabbit Antibody	Abmart Pharmaceutical Technology Co., Ltd. (cat. no. TA4331)
PPARγ Rabbit Antibody	Abmart Pharmaceutical Technology Co., Ltd. (cat. no. TD6073)
p-PPARγ (Ser273) Rabbit Antibody	Abmart Pharmaceutical Technology Co., Ltd. (cat. no. TA3675)

HRP, horseradish peroxidase; mAb, monoclonal antibody; p-, phosphorylated; pAb, polyclonal antibody; PGBD5, piggyBac transportable element derived 5; PPAR, peroxisome proliferator-activated receptor.

resistance gene sequence; therefore, to further eliminate the influence of wild-type cells on subsequent experiments, 2 μg/ml puromycin (Dalian Meilun Biology Technology Co., Ltd.) was used to screen the cells. After undergoing more than three sub-culturing cycles, the cell population predominantly exhibited antibiotic resistance. Western blotting and RT-qPCR were used to evaluate the protein and mRNA expression levels of PGBD5 in cells infected with sh-PGBD5 and sh-NC.

Transwell assay. Precooled FBS-free medium was added to the lower chamber of a 24-well Transwell chamber (Corning Life Sciences) to evenly hydrate the basement membrane, and precooled FBS-free medium was also used to dilute Matrigel (Corning Life Sciences) at a dilution ratio of 7:1. Subsequently, 100 μl prepared Matrigel was added to the upper chamber, and the chamber was incubated at 37˚C for 1 h to solidify the matrix. The Transwell chamber was then removed from the incubator, the medium in the upper chamber was aspirated carefully, and 600 μl complete medium supplemented with 10% FBS was added to the lower chamber. A certain cell suspension volume was prepared, and 200 μl of the suspension, containing a cell density of $1x10^5$ cells/ml, was added evenly to each well in the upper chamber. After 24 h at 37˚C, the chamber was removed, and the culture medium, cells and Matrigel in the upper chamber were carefully wiped with a cotton swab. Cells that had migrated to the lower chamber were fixed with 600 μl 4% paraformaldehyde (Beijing Solarbio Science & Technology Co., Ltd.) for 30 min at room temperature. After fixation, the chamber was stained with crystal violet solution (Beijing Solarbio Science & Technology Co., Ltd.) for 30 min at room temperature. Finally, the chamber was washed three times with PBS. After air-drying, five high-power fields were randomly selected under a light microscope for observing and counting the cells. Matrigel was added to the upper chamber for the invasion assay, whereas it was not added to the upper chamber for the migration assay.

Cell apoptosis analysis. A172, U251 and U87 cells were collected by digesting and centrifuging. After the binding buffer was diluted with deionized water at a 3:1 ratio, the cells were resuspended and the concentration was adjusted to $4x10^6$/ml. In a 5-ml flow tube, 100 μl cell suspension was added along with 5 μl Annexin V/PE. After pipetting and mixing, the suspension was incubated at room temperature in the dark for 5 min. Subsequently, the suspension was stained with 10 μl 20 μg/ml 7AAD and 400 μl PBS in the dark for 15 min at room temperature. An Annexin V-PE/7-AAD apoptosis detection kit (Nanjing KeyGen Biotech Co., Ltd.) was used, followed by detection using a Novocyte 2060r Flow Cytometer (ACEA Bisociences; Agilent Technologies, Inc.) and data analysis using FlowJo 10.4 (FlowJo LLC).

Cell cycle distribution analysis. A172, U251 and U87 cells were collected by digesting and centrifuging. Next, 500 μl 1X staining buffer with RNase A (25 μg/ml) was added to resuspend the cells and 5 μl PI dye was added to label the cells in the dark for 30 min at 37˚C. For this assay, a Cell Cycle Detection Kit (Beijing 4A Biotech Co., Ltd.) was used for cell cycle analysis, followed by detection using a Novocyte 2060r Flow Cytometer and data analysis using FlowJo 10.4.

Tumor xenograft assay. Nude BALB/c mice (age, 6 weeks; male) were purchased from the Animal Experiment Center at Kunming Medical University. The mice were raised in a controlled temperature (20±2˚C) and 50-60% humidity under a 12-h light/dark cycle, and food and water were provided *ad libitum*. The nude mice were randomly divided into two groups (n=5/group; weight, 18-21 g): U87-sh-PGBD5 and

U87-sh-NC groups. The U87-sh-PGBD5 and U87-sh-NC cells were cultured separately, and when the cells were in the logarithmic growth phase, they were digested and centrifuged at 200 x g for 5 min at 4˚C, resuspended in sterile PBS and the cell suspension concentration was adjusted to $2.0x10^6$ cells/100 μl. Subsequently, 100 μl cell suspension was injected subcutaneously into the right armpit of the nude mice. The tumors were checked daily, and the measurements of the longest and shortest diameters were recorded once a week using vernier calipers. The tumor volume was calculated as follows: Tumor volume=0.52 x L x W^2; where L is the longest diameter of the tumor and W is the shortest diameter of the tumor. After 5 weeks of monitoring, or upon reaching humane endpoints (defined as mice losing 20% body weight or exhibiting moribund behavior), the mice were sacrificed. Prior to cervical dislocation, the mice were deeply anesthetized with 5% isoflurane to minimize any potential pain or distress during the procedure. The tumors were then collected, and the tumor volume curve was prepared.

Immunohistochemistry. Nude mouse subcutaneous tumors were immediately fixed in 4% paraformaldehyde for 48 h at 4˚C, dehydrated in graded alcohol and xylene, embedded in paraffin and sliced into 3-μm serial sections. The samples were heated in an oven for 30 min at 60˚C, and were then dewaxed in different concentrations (100, 95 and 75%) of xylene (10 min) and graded alcohol (2 min). After rinsing with tap water, the sections were immersed in EDTA antigen retrieval solution (MXB Biotechnologies) for 3 min at 95˚C and allowed to cool naturally. Subsequently, 3% H_2O_2 was added to the sections at room temperature for 15 min, followed by washing three times with PBS. The sections were first blocked for nonspecific binding using 5% normal goat serum (cat. no. 566380; MilliporeSigma) in PBS for 20 min at room temperature, then incubated with Ki67 antibody at a dilution of 1:100 (MXB Biotechnologies; cat. no. RMA-0731) at 26˚C for 75 min and were washed three times with PBS, after which, they were incubated with horseradish peroxidase-conjugated goat anti-mouse IgG antibody (Dako; Agilent Technologies, Inc.) for 30 min and then washed three times with PBS. Subsequently, the sections were incubated with a freshly prepared DAB staining solution (MXB Biotechnologies) for 15 min at room temperature. This was followed by washing three times with PBS and incubation with hematoxylin solution for 14 sec at room temperature. The sections were then treated with hydrochloric acid and alcohol differentiation solution, and rinsed with tap water. Finally, the sections were dehydrated with graded ethanol, permeabilized with xylene, mounted with neutral balm and a coverslip was placed over the sections. Subsequently, images were captured under a light microscope. For hematoxylin and eosin staining, sections were stained with hematoxylin (0.1% w/v in water) for 4 min at room temperature to highlight the nuclei, followed by a brief rinse in running tap water to remove excess stain. Subsequently, eosin (1% w/v in water) staining was applied for 2 min at room temperature to visualize cytoplasmic and extracellular matrix components. After staining, sections were dehydrated, cleared, and mounted with a coverslip using a xylene-based mounting medium. Stained sections were examined under a light microscope.

Transcriptomics study. The sh-NC and sh-PGBD5 A172 and U87 cell groups were simultaneously cultured in T25 culture flasks for transcription analysis. When the cell flasks reached 100% confluence, RNA was extracted from the cells using RNAIso Plus (Takara Biotechnology, Ltd.; cat. no. 9108). RNA sequencing was performed at MajorBiotech. After quality verification with a BioAnalyzer 2100 (Agilent Technologies, Inc.), RNA libraries at a final concentration of 300 pM were sequenced using an Illumina NovaSeq 6000 SP Reagent kit v1.5 (300 cycles; cat. no. 20028400; Illumina, Inc.) in 150 bp paired-end reads. Reference gene source: *Homo sapiens*; reference genome version: GRCh38; reference genome source: http://asia.ensembl.org/Homo_sapiens/Info/Index. The clean reads of these samples were compared with the designated reference genome. Based on the quantitative expression results, differential gene analyses were performed between groups to identify the differentially expressed genes between each pair. DESeq2 software (Bioconductor, Inc.; https://bioconductor.org/packages/release/bioc/html/DESeq2.html) was used for differential gene analysis, and the screening threshold was: $\log_2FC \geq 1/\log_2FC \leq -1$, Padjust <0.05. The P-values were adjusted for multiple testing using the Benjamini-Hochberg method. Principal component analysis (PCA) was employed to reduce the dimensionality of the transcriptomic data, enabling the identification of the principal components within the dataset. Gene Ontology (GO) and Kyoto Encyclopedia of Genes and Genomes (KEGG) pathway analyses were performed. GO analysis was performed using DAVID (https://david.ncifcrf.gov) to understand the functions of the identified genes. KEGG pathway analysis was performed using KAAS (https://www.genome.jp/kaas-bin/kaas_main) to identify which pathways the genes were involved in.

Statistical analysis. The data in the present study are presented as mean ± standard deviation for continuous variables, and were analyzed using SPSS 22.0 statistical software (IBM Corp.). The experiments were repeated a minimum of three times. Comparisons between two groups were performed using a paired or unpaired Student's t-test. Multi-group comparisons were performed using one-way ANOVA with the Tukey's multiple comparison test. P<0.05 was considered to indicate a statistically significant difference.

Results

PGBD5 expression in glioma cells and tissues. The relative protein and mRNA expression levels of PGBD5 were significantly elevated in glioma tissues compared with those in para-cancerous tissues (P<0.01; Figs. 1A and C, and S1A). The relative protein and mRNA expression levels of PGBD5 were also significantly higher in glioma cell lines (A172, U251 and U87) compared with those in NHAs (P<0.001; Figs. 1B and D, and S1B). The results suggested that the protein and mRNA expression levels of PGBD5 were increased in both glioma tissues and cell lines.

Lentivirus-mediated PGBD5 silencing in glioma cells. The detection of GFP staining indicated successful lentiviral infection (Fig. 2A). In addition, the protein (Figs. 2B and S1C) and mRNA (Fig. 2C) expression levels

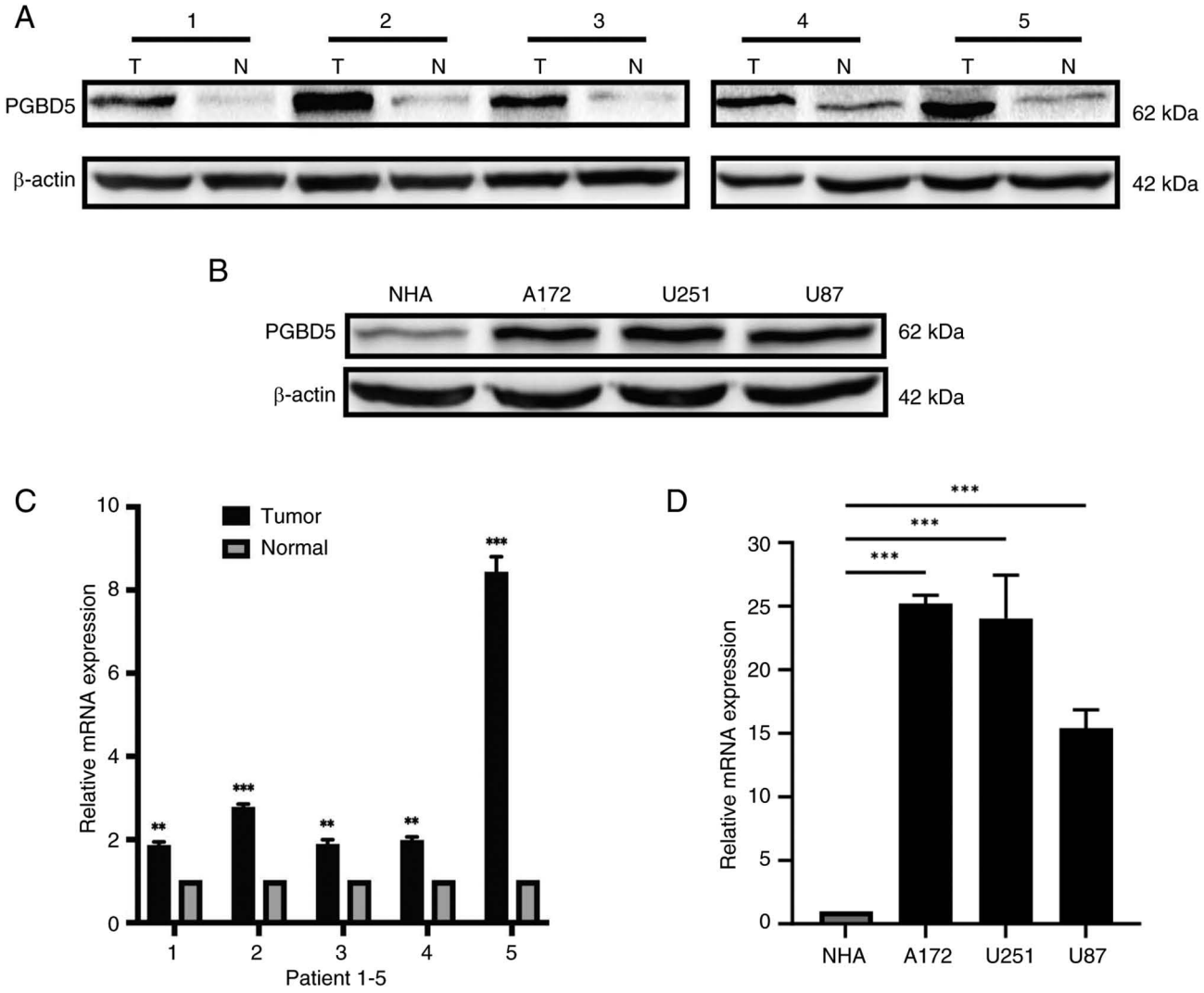

Figure 1. Increased expression of PGBD5 is associated with glioma development. (A) Protein expression in five cases of glioma tissues and adjacent non-cancerous tissues. (B) Protein expression in NHAs and glioma cell lines (A172, U251 and U87). mRNA expression levels were examined in (C) glioma tissues and para-cancerous tissues, and (D) NHAs and glioma cell lines (A172, U251 and U87). β-actin was used as the protein loading control. The experiments were repeated three times. **P<0.01, ***P<0.001 vs. T or as indicated. N, normal; NHA, normal human astrocyte; PGBD5, piggyBac transportable element derived; T, tumor.

of PGBD5 were markedly decreased in A172, U251 and U87 glioma cells in the sh-PGBD5 group, compared with those in the sh-NC group (P<0.001). These results suggested that lentivirus-mediated PGBD5 silencing was successful in glioma cells.

Effects of PGBD5 knockdown on glioma cells. The knockdown of PGBD5 inhibited glioma cell migration (Fig. 3A and B) and invasion (Fig. 3C and D) compared with those in the sh-NC group (P<0.001). In addition, PGBD5 knockdown significantly induced the apoptosis of glioma cells compared with that in the sh-NC group (P<0.05; Fig. 4A and B). The knockdown of PGBD5 could also cause glioma cell cycle arrest in the G_2/M phase (P<0.05; Fig. 4D and E). PGBD5 knockdown not only promoted the expression levels of apoptosis-related proteins, such as Bax and cleaved caspase-3, but also inhibited the expression levels of anti-apoptotic proteins and carcinogenic cell cycle regulators, such as Bcl-2, CDK1 and cyclin B1 (Figs. 4C and F, and S1D-I).

PGBD5 knockdown inhibits glioma growth in vivo. The growth rate and volume of the subcutaneous tumors in nude mice from the sh-PGBD5 group were significantly reduced compared with those in the sh-NC group (P<0.01; Fig. 5A-C). Hematoxylin and eosin staining was performed to analyze the subcutaneous tumors of nude mice, which revealed characteristic histological features associated with tumor growth, such as increased cellularity, irregular nuclear morphology and aberrant tissue architecture (Fig. 5D). In addition, immunohistochemical analysis showed that, in the sh-PGBD5 group, the expression levels of Ki67 were inhibited compared with those in the sh-NC group *in vivo* (Figs. 5E and S1N), which may have markedly restricted the growth of subcutaneous tumors.

PGBD5 promotes glioma progression via the PPAR signaling pathway. PCA was conducted on four groups of samples, the separation of the four groups underscores the unique transcriptomic signatures, highlighting the potential for underlying biological differences caused by PGBD5 knockdown (Fig. 6A).

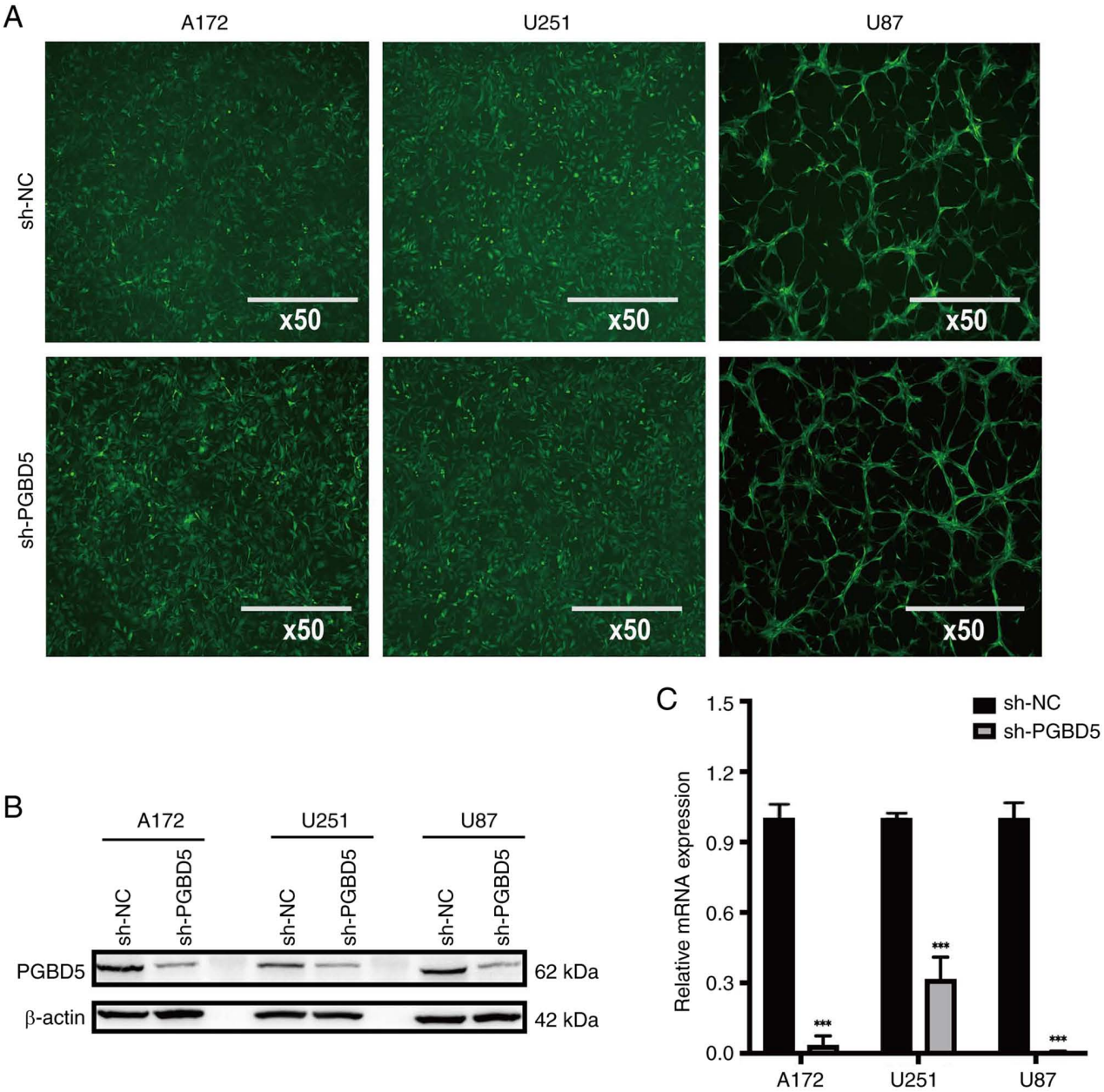

Figure 2. Verification of the effect of lentiviral infection. (A) Enhanced green fluorescent protein-carrying lentivirus successfully infected glioma cell lines, showing green fluorescence under a fluorescence microscope. (B) PGBD5 protein expression was detected in both sh-PGBD5 and sh-NC groups. (C) Detection of the mRNA expression levels of PGBD5 in sh-PGBD5 and sh-NC groups. β-actin was used as the protein loading control. The experiments were repeated three times. ***P<0.001 vs. sh-NC. NC, negative control; PGBD5, piggyBac transportable element derived; sh, short hairpin.

Venn analysis revealed that after PGBD5 knockdown, 1,230 genes were differentially expressed in the A172 cell group, and 1,308 genes were differentially expressed in the U87 cell group, of which 242 genes overlapped (Fig. 6B). Furthermore, transcriptome analysis revealed that compared with that in the sh-NC group, Knocking down PGBD5 significantly affected 'cellular metabolic process' (GO:0044237) and the 'PPAR signaling pathway' (KEGG:03320), indicating a crucial role of PGBD5 in regulating metabolic processes and signaling mechanisms related to PPAR (Fig. 6C-F). In contrast with that in the sh-NC group, the phosphorylated and total expression levels of PPARδ and PPARγ were increased in the sh-PGBD5 group (Figs. 6G and S1J-M), both indicating enhanced activity of PPARδ and PPARγ. Furthermore, the phosphorylated and total expression levels of PPARδ were increased in response to PGBD5 knockdown in A172 and U87 cells, but not in U251 cells (Fig. 6G). *In vivo* experiments involving subcutaneous tumors in nude mice revealed that PPARγ and PPARδ levels in the sh-PGBD5 group were markedly higher than those in the sh-NC group (P<0.05; Figs. 6H, and S1O-P). Fig. S1 shows statistical analysis of all western blots. A graphical overview of the research findings can be found in Fig. 7.

Discussion

In the present study, the biological function and molecular mechanism of action of PGBD5 in glioma were assessed using RT-qPCR, western blotting, Transwell assay, flow cytometry

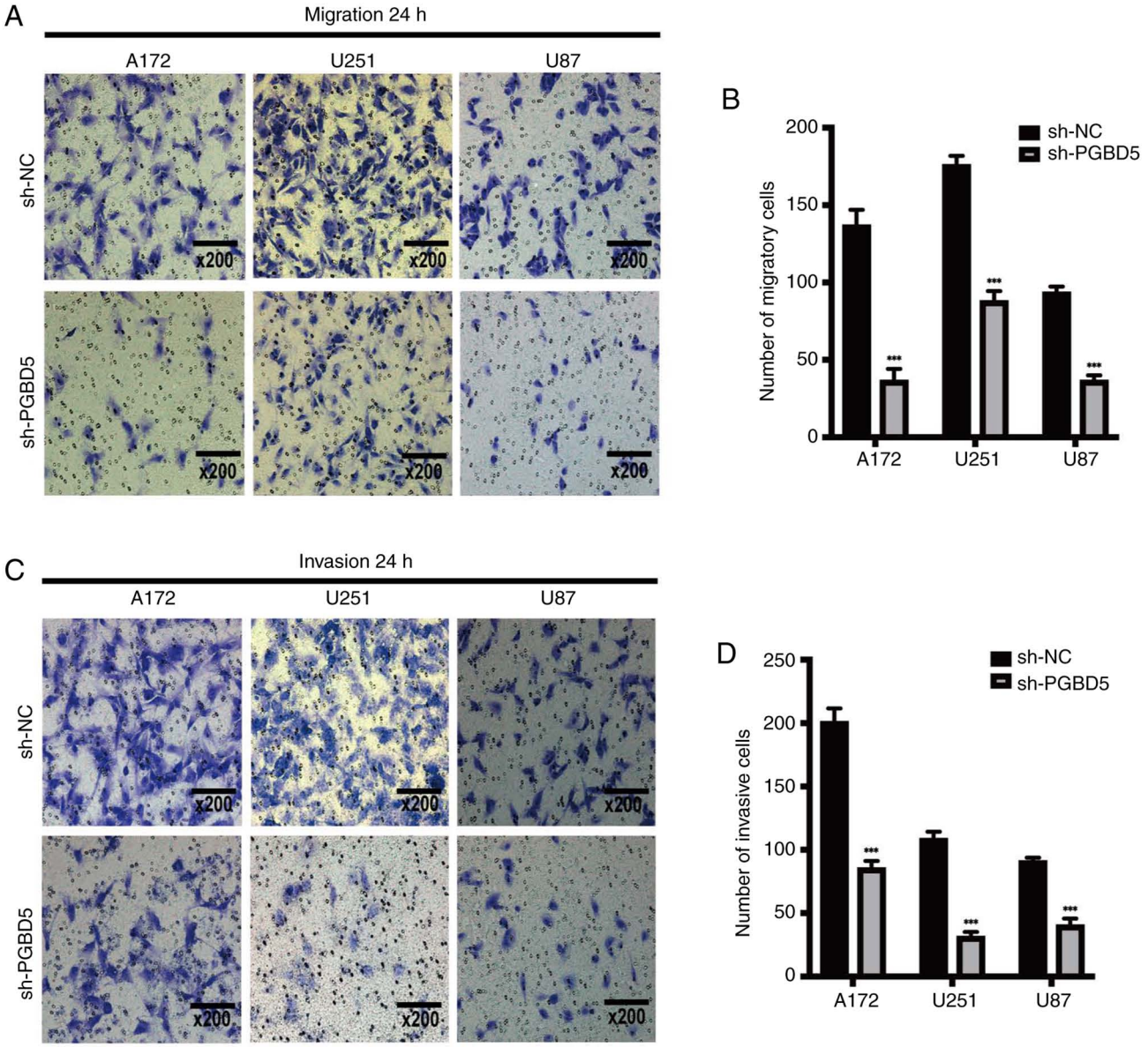

Figure 3. PGBD5 knockdown can inhibit the migration and invasion of glioma cells. (A) Transwell assay, with (B) statistical analysis, for assessment of the migration of glioma cells. (C) Transwell assay, with (D) statistical analysis, for assessing the invasion of glioma cells. The experiments were repeated three times. ***P<0.001 vs. sh-NC. NC, negative control; PGBD5, piggyBac transportable element derived; sh, short hairpin.

and histopathology. The results revealed that PGBD5 was upregulated in glioma tissues and cell lines, and *in vitro* experiments revealed that, after PGBD5 knockdown, some of the biological functions of glioma cells were affected, which could inhibit the growth of glioma *in vivo*. Furthermore, transcriptomic analysis demonstrated that PGBD5 knockdown could activate the PPAR signaling pathway and upregulate the expression of PPAR-related proteins, thus exerting an anticancer effect.

Glioma is a common tumor originating from glial cells, which exhibits a high degree of malignancy. The malignant behavior of glioma may be related to the expression of multiple genes and various signaling pathways, such as TP53, EGFR and IDH1 (43). At present, surgery with radiotherapy and chemotherapy remains the major treatment strategy for glioma. Although numerous potential therapeutic targets have been identified, additional clinical investigation is required to determine effective treatment strategies (44). PGBD5 is a member of the piggyBac transposon family, and the cell transformation it induces has been linked to the occurrence of chromosome deletion, inversion and translocation (28). In our preliminary unpublished experiments, it was observed that PGBD5 overexpression in tumor-bearing mice and glioma cells did not significantly alter tumor progression or severity, whereas knocking down PGBD5 substantially reduced tumor size. The lack of impact from PGBD5 overexpression may be due to high endogenous levels of PGBD5 in the models, thus resulting in a saturation effect, or it may indicate that the function of this gene is context-dependent and influenced by other factors. Given these findings and the complex nature of glioma biology, the present study focused on the effects of PGBD5 knockdown.

PPAR is a transcription factor from the nuclear hormone receptor superfamily that is activated by fatty acids and regulates energy metabolism. PPAR is also expressed in immune

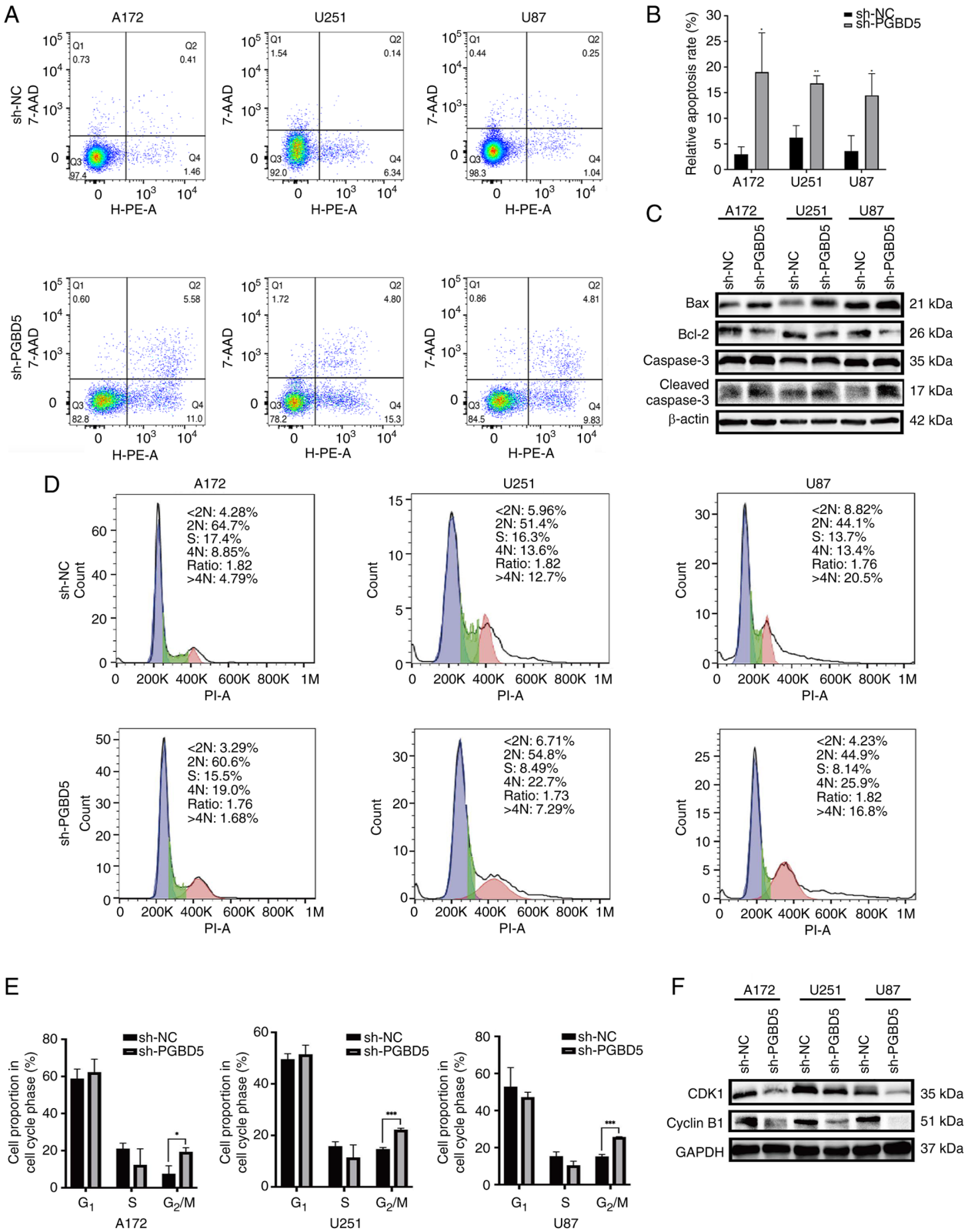

Figure 4. Effects of PGBD5 knockdown on the apoptosis of glioma cells. (A and B) Effects of PGBD5 knockdown on the cell cycle progression of glioma cells. (D and E) Apoptosis and cell cycle distribution of glioma cells were detected using flow cytometry. Western blotting showed the expression levels of (C) apoptosis-related proteins (Bax, Bcl-2 and caspase-3) and (F) cell cycle-related proteins (CDK1 and cyclin B1) in glioma cell lines after PGBD5 knockdown. β-actin or GAPDH were used as the protein loading controls. The experiments were repeated three times. *P<0.05, **P<0.01, ***P<0.001 vs. sh-NC or as indicated. NC, negative control; PGBD5, piggyBac transportable element derived; sh, short hairpin.

cells and serves an important role in their differentiation (45). Because of its strong pharmacological activity, PPAR has been identified as a therapeutic target in multiple diseases, such as metabolic disorders, cardiovascular diseases and inflammatory diseases (46). An increasing body of evidence has shown that PPAR exerts a key regulatory effect on various aspects of

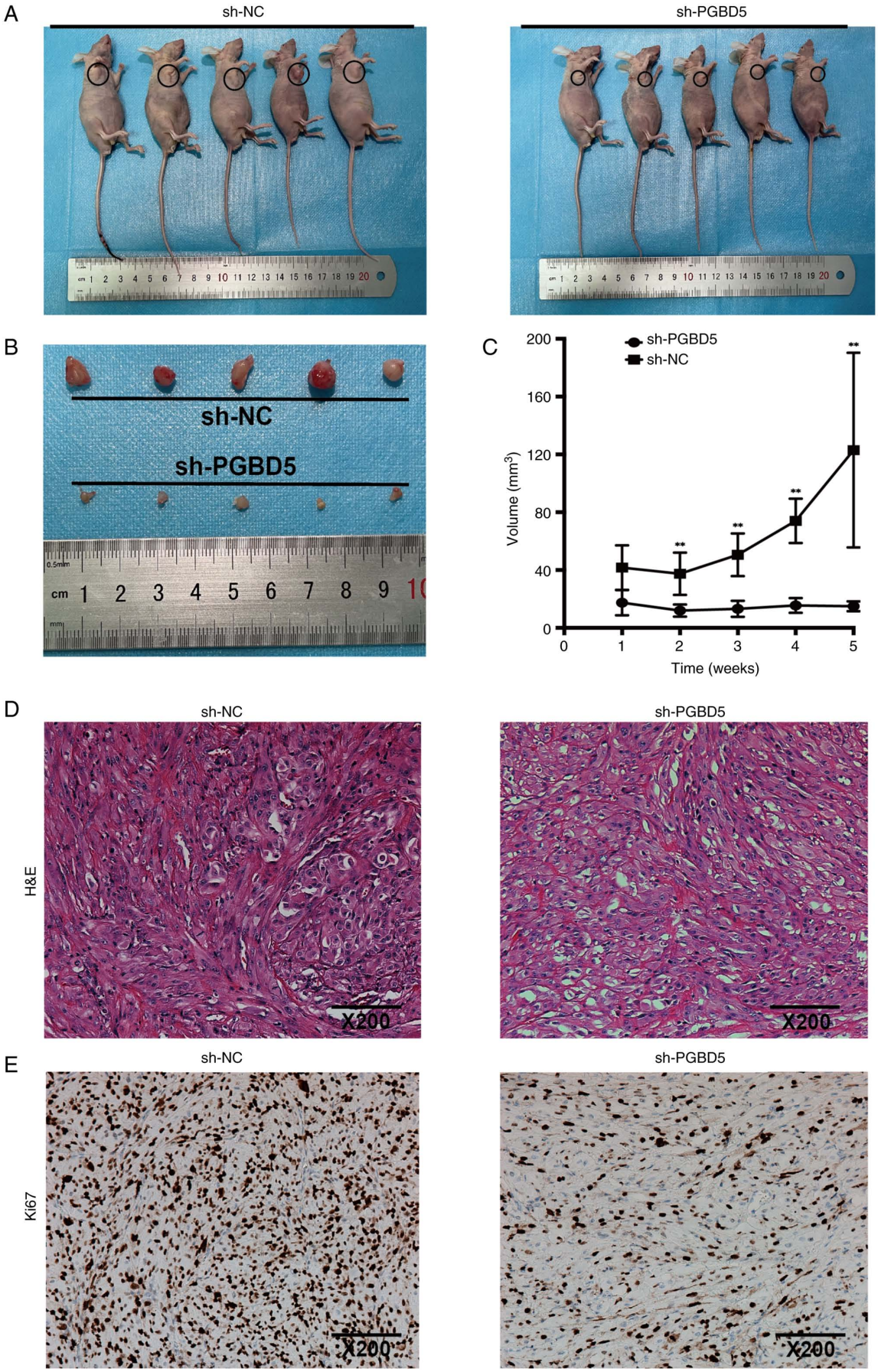

Figure 5. Knockdown of PGBD5 inhibits glioma growth *in vivo*. (A) Images of nude mice before subcutaneous tumor dissection and (B) images of dissected tumors (n=5/group). (C) Growth curve of the transplanted tumors in nude mice. **P<0.01 vs. sh-PGBD5. (D) H&E staining of tumor tissues. (E) Differential expression of Ki67 within tumor samples, as detected using immunohistochemistry. H&E, hematoxylin and eosin; NC, negative control; PGBD5, piggyBac transportable element derived; sh, short hairpin.

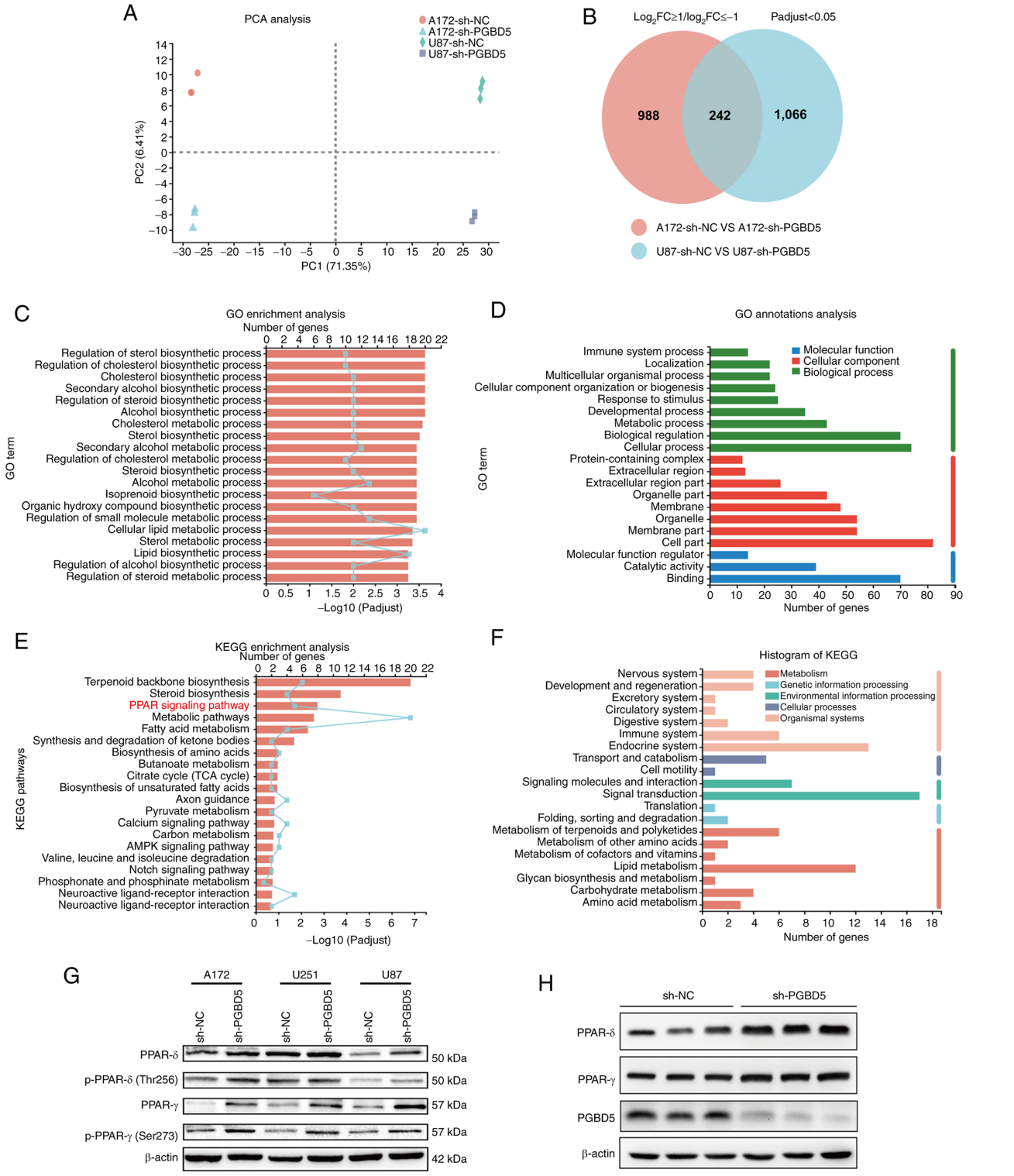

Figure 6. PPAR is involved in the effect of PGBD5 on the occurrence and development of glioma. (A) PCA of data from four groups of samples. (B) Venn diagram showed 1,230 altered genes in the A172 cells and 1,308 in the U87 cells, among which 242 gene alterations were overlapping. (C) GO enrichment analyses and (D) GO annotation analyses of differentially expressed genes revealed significant associations with cellular metabolic process. (E) KEGG enrichment analyses and (F) KEGG enrichment analyses of differentially expressed genes revealed significant associations with the PPAR signaling pathway. (G) Western blotting was performed to detect PPAR-related protein expression. β-actin was used as the protein loading control. The experiments were repeated three times. (H) PGBD5, PPARγ and PPARδ levels in *in vivo* subcutaneous tumors after PGBD5 knockdown. GO, Gene Ontology; KEGG, Kyoto Encyclopedia of Genes and Genomes; NC, negative control; p-, phosphorylated; PCA, principal component analysis; PGBD5, piggyBac transportable element derived; PPAR, peroxisome proliferator-activated receptor; sh, short hairpin.

immunity, inflammation, vascular function, oxidative stress, cell proliferation, differentiation, development, apoptosis and cancer (47,48).

In several studies, PPAR, as a regulator, has been confirmed to serve important roles in the proliferation and differentiation of cancer cells (41,49). Because PPAR occasionally acts

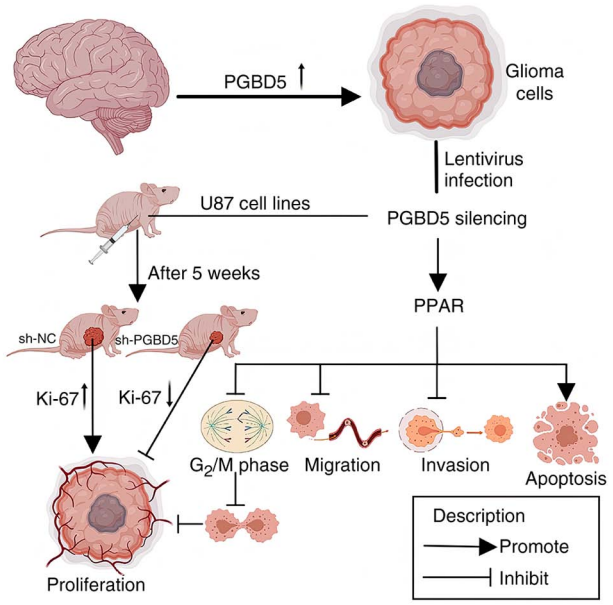

Figure 7. Graphical overview of the research findings. NC, negative control; PGBD5, piggyBac transportable element derived 5; PPAR, peroxisome proliferator-activated receptor; sh, short hairpin.

as a carcinogen and a suppressor in different tumor types, there may be conflicting results from different studies (50,51). Furthermore, PPARδ not only maintains metabolic activity in peripheral organs and tissues (52), but also exhibits high expression in the brain (53). Other studies have shown that the absence of PPARδ expression in mice can cause defects in brain development (54). PPAR expression is also associated with some age-related diseases, and PPARγ has a role as a biomarker in patients with cerebral ischemia (55). It may also serve an important role in the inhibition of tumors of neuroectodermal origin, since PPARδ and its ligand erucic acid have been shown to exert antitumor, neuroprotective and myelinating effects in neuroblastoma, glioblastoma and Parkinson's disease (56). Erucic acid at therapeutic concentration can also reduce the proliferation of C6 glioma cells *in vitro* and induce the death of C6 glioma cells (57). A previous study also showed that PPAR induces a synergistic effect on the differentiation of C6 glioma cells into oligodendrocytes (58). Moreover, PPARδ may promote the expression of both PPARα and PPARγ to increase the expression of oligodendrocyte-specific markers and enzymes necessary for myelin synthesis in C6 glioma cells (58). Two major classes of agonists of PPARγ, including thiazolidinedione and non-thiazolidinedione, can block the migration and invasion of glioma cells and other highly-invasive solid tumors; however, the specific mechanism remains unclear (59). Other studies have also revealed that the PPAR-mediated signaling pathway and gene expression defects may affect the normal expression and induction of catalase in malignant glioma (60,61); however, further investigation showed that PPAR agonists can significantly improve the expression level and activity of catalase in normal astrocytes, but exert no significant effect on glioma cells. Nevertheless, this suggests that PPAR agonists may serve as a potential drug for glioma treatment (60). Another study on clinical glioma tissues demonstrated that PPARγ exhibits positive expression rates of 94.1% in LGG and 39.6% in HGG, and its expression is closely related to microvessel density; thus, PPARγ may be involved in the regulation of angiogenesis in glioma (62).

The mechanisms through which PGBD5 knockdown influences the PPAR pathway may involve various cellular processes. It is plausible that PGBD5 affects the stability and transcriptional activity of PPARs or their co-regulators through direct or indirect interactions. Alterations in PGBD5 could lead to changes in chromosomal structure or gene expression profiles, thereby modulating the PPAR pathway. Additionally, as PGBD5 influences chromosomal stability, its knockdown may lead to a more stable genomic environment, reducing the mutations or alterations that could lead to dysregulated PPAR activity, a common occurrence in cancer cells.

The present study has numerous limitations. First, the sample size of glioma tissues was relatively low, and a study with a larger sample size is needed. The most notable limitation was the lack of rescue experiments for PGBD5 gene expression or PPAR signaling, which will be focused upon in future research. The potential protein-protein interaction between PGBD5 and PPAR also needs further investigation. Additionally, the specific mechanism through which the PPAR pathway promotes glioma cell migration and invasion was not fully elucidated within the current study. In future studies, we aim to focus on assessing the signaling cascades downstream of PPAR activation. This would involve a detailed analysis of the PPAR-responsive elements within the glioma genome, and how agonists modulate the transcription of genes involved in cell motility, adhesion and extracellular matrix remodeling, which are critical for migration and invasion.

Although PGBD5 is a highly conserved gene, it has been shown that it has long lost its transposase activity (63); thus, its complete knockout by genome editing technologies such as CRISPR-Cas9 will exert a limited effect on the organism. Establishing a rat model of intracranial *in situ* tumor, and observing the changes and primary blood indicators following PGBD5 gene knockout are the next steps. This will help eliminate the limitations caused by immunosuppression in nude mice to a certain extent. Given the molecular diversity and complexity of glioma, understanding individual molecular targets such as PGBD5 can lead to more personalized and effective treatments. Patients whose glioma exhibits significant upregulation of PGBD5 may benefit from therapies specifically designed to target this gene, leading to more tailored and potentially more effective treatment strategies. In our future work, we aim to develop drugs or gene therapies that can effectively target PGBD5. This may involve screening for small molecules that inhibit PGBD5, developing RNA interference technologies or other gene-editing techniques, such as CRISPR, to knockdown or edit the gene in tumor cells.

In conclusion, the present study demonstrated that the expression of PGBD5 was upregulated in glioma tissues and cells. Knockdown of PGBD5 expression exerted an anticancer effect mediated by the promotion of PPAR expression *in vitro*, which not only accelerated the apoptosis of glioma cells, but also inhibited their migration, invasion and induced cell cycle arrest. PGBD5 silencing could also significantly restrict tumor growth *in vivo*. The present study first evaluated the biological role of PGBD5 in glioma and preliminarily explored its related molecular mechanisms. To some extent, the findings of the

current study provided a theoretical reference for exploring novel therapeutic targets in human glioma.

Acknowledgements

Not applicable.

Funding

This research was supported by the Xingdian Talent Support Plan Project (grant no. XDYC-QNRC-2022-0320) and the Joint Projects of Kunming University of Science and Technology and Medical Science (grant no. KUST-KH2023028Y).

Availability of data and materials

The data generated in the present study may be found in the BioProject database under accession number PRJNA953025 or at the following URL: https://www.ncbi.nlm.nih.gov/bioproject/PRJNA953025/

Authors' contributions

PL, JY and SZ designed the study. PL, JY and LJ carried out the experiments. JD, SY and CL participated in the data analysis. PL, JY and SZ wrote the manuscript. JD, SY and CL revised the manuscript critically for important intellectual content. PL and SZ confirm the authenticity of all the raw data. All authors read and approved the final manuscript.

Ethics approval and consent to participate

The use of NHAs, paired tumor tissues and para-cancerous tissues were approved by the Ethics Committee of Kunming University of Science and Technology School of Medicine (approval no. KMUST-MEC-092). All enrolled patients provided written informed consent. The animal experiments were conducted in accordance with the national legislation and associated guidelines, and the procedures were approved by the Ethics Committee of Kunming University of Science and Technology School of Medicine [approval no. PZWH (DIAN) K2021-0021]. The study was conducted in accordance with the guidelines of The Declaration of Helsinki.

Patient consent for publication

Written informed consent has been obtained from the patients to publish this paper.

Competing interests

The authors declare that they have no competing interests.

References

1. Louis DN, Perry A, Wesseling P, Brat DJ, Cree IA, Figarella-Branger D, Hawkins C, Ng HK, Pfister SM, Reifenberger G, *et al*: The 2021 WHO classification of tumors of the central nervous system: A summary. Neuro Oncol 23: 1231-1251, 2021.
2. Weller M and Le Rhun E: How did lomustine become standard of care in recurrent glioblastoma? Cancer Treat Rev 87: 102029, 2020.
3. Duffau H and Taillandier L: New concepts in the management of diffuse low-grade glioma: Proposal of a multistage and individualized therapeutic approach. Neuro Oncol 17: 332-342, 2015.
4. Campian J and Gutmann DH: CNS tumors in neurofibromatosis. J Clin Oncol 35: 2378-2385, 2017.
5. Lapointe S, Perry A and Butowski NA: Primary brain tumours in adults. Lancet 392: 432-446, 2018.
6. Lin L, Cai J and Jiang C: Recent advances in targeted therapy for glioma. Curr Med Chem 24: 1365-1381, 2017.
7. Gottesman MM, Robey RW and Ambudkar SV: New mechanisms of multidrug resistance: An introduction to the cancer drug resistance special collection. Cancer Drug Resist 6: 590-595, 2023.
8. Liu A, Jiang B, Song C, Zhong Q, Mo Y, Yang R, Chen C, Peng C, Peng F and Tang H: Isoliquiritigenin inhibits circ0030018 to suppress glioma tumorigenesis via the miR-1236/HER2 signaling pathway. MedComm (2020) 4: e282, 2023.
9. Tang H, Liu Q, Liu X, Ye F, Xie X, Xie X and Wu M: Plasma miR-185 as a predictive biomarker for prognosis of malignant glioma. J Cancer Res Ther 11: 630-634, 2015.
10. Yu Q, Fu W, Fu Y, Ye W, Yan H, Yu Z, Li R, Cai Y, Chen Y, Wang L, *et al*: BNIP3 as a potential biomarker for the identification of prognosis and diagnosis in solid tumours. Mol Cancer 22: 143, 2023.
11. Zhang B, Zhao J, Wang Y, Xu H, Gao BO, Zhang G, Han B, Song G, Zhang J and Meng W: CHRM3 is a novel prognostic factor of poor prognosis and promotes glioblastoma progression via activation of oncogenic invasive growth factors. Oncol Res 31: 917-927, 2023.
12. Cordaux R and Batzer MA: The impact of retrotransposons on human genome evolution. Nat Rev Genet 10: 691-703, 2009.
13. Smit AF: Interspersed repeats and other mementos of transposable elements in mammalian genomes. Curr Opin Genet Dev 9: 657-663, 1999.
14. Muñoz-López M and García-Pérez JL: DNA transposons: Nature and applications in genomics. Curr Genomics 11: 115-128, 2010.
15. Schrader L and Schmitz J: The impact of transposable elements in adaptive evolution. Mol Ecol 28: 1537-1549, 2019.
16. Percharde M, Sultana T and Ramalho-Santos M: What doesn't kill you makes you stronger: Transposons as dual players in chromatin regulation and genomic variation. Bioessays 42: e1900232, 2020.
17. Morales ME, Servant G, Ade C and Roy-Engel AM: Altering genomic integrity: Heavy metal exposure promotes transposable element-mediated damage. Biol Trace Elem Res 166: 24-33, 2015.
18. Deniz Ö, Frost JM and Branco MR: Regulation of transposable elements by DNA modifications. Nat Rev Genet 20: 417-431, 2019.
19. Saleh A, Macia A and Muotri AR: Transposable elements, inflammation, and neurological disease. Front Neurol 10: 894, 2019.
20. Burns KH: Our conflict with transposable elements and its implications for human disease. Annu Rev Pathol 15: 51-70, 2020.
21. Payer LM and Burns KH: Transposable elements in human genetic disease. Nat Rev Genet 20: 760-772, 2019.
22. Yusa K: piggyBac transposon. Microbiol Spectr 3: MDNA3-0028-2014, 2015.
23. Helou L, Beauclair L, Dardente H, Piégu B, Tsakou-Ngouafo L, Lecomte T, Kentsis A, Pontarotti P and Bigot Y: The piggyBac-derived protein 5 (PGBD5) transposes both the closely and the distantly related piggyBac-like elements Tcr-pble and Ifp2. J Mol Biol 433: 166839, 2021.
24. Majumdar S, Singh A and Rio DC: The human THAP9 gene encodes an active P-element DNA transposase. Science 339: 446-448, 2013.
25. Henssen AG, Henaff E, Jiang E, Eisenberg AR, Carson JR, Villasante CM, Ray M, Still E, Burns M, Gandara J, *et al*: Genomic DNA transposition induced by human PGBD5. Elife 4: e10565, 2015.
26. Pavelitz T, Gray LT, Padilla SL, Bailey AD and Weiner AM: PGBD5: A neural-specific intron-containing piggyBac transposase domesticated over 500 million years ago and conserved from cephalochordates to humans. Mob DNA 4: 23, 2013.
27. Sarkar A, Sim C, Hong YS, Hogan JR, Fraser MJ, Robertson HM and Collins FH: Molecular evolutionary analysis of the widespread piggyBac transposon family and related 'domesticated' sequences. Mol Genet Genomics 270: 173-180, 2003.
28. Henssen AG, Koche R, Zhuang J, Jiang E, Reed C, Eisenberg A, Still E, MacArthur IC, Rodríguez-Fos E, Gonzalez S, *et al*: PGBD5 promotes site-specific oncogenic mutations in human tumors. Nat Genet 49: 1005-1014, 2017.

29. Xie W, Zeng Y, Hu L, Hao J, Chen Y, Yun X, Lin Q and Li H: Based on different immune responses under the glucose metabolizing type of papillary thyroid cancer and the response to anti-PD-1 therapy. Front Immunol 13: 991656, 2022.
30. Yu Z, Du M and Lu L: A novel 16-genes signature scoring system as prognostic model to evaluate survival risk in patients with glioblastoma. Biomedicines 10: 317, 2022.
31. Phua WWT, Wong MXY, Liao Z and Tan NS: An aPPARent functional consequence in skeletal muscle physiology via peroxisome proliferator-activated receptors. Int J Mol Sci 19: 1425, 2018.
32. Montaigne D, Butruille L and Staels B: PPAR control of metabolism and cardiovascular functions. Nat Rev Cardiol 18: 809-823, 2021.
33. Wang YX: PPARs: Diverse regulators in energy metabolism and metabolic diseases. Cell Res 20: 124-137, 2010.
34. Mirza AZ, Althagafi II and Shamshad H: Role of PPAR receptor in different diseases and their ligands: Physiological importance and clinical implications. Eur J Med Chem 166: 502-513, 2019.
35. Tan Y, Wang M, Yang K, Chi T, Liao Z and Wei P: PPAR-alpha modulators as current and potential cancer treatments. Front Oncol 11: 599995, 2021.
36. Dong YW, Wang XP and Wu K: Suppression of pancreatic carcinoma growth by activating peroxisome proliferator-activated receptor gamma involves angiogenesis inhibition. World J Gastroenterol 15: 441-448, 2009.
37. Zhang N, Li G, Li X, Xu L and Chen M: Circ5379-6, a circular form of tumor suppressor PPARα, participates in the inhibition of hepatocellular carcinoma tumorigenesis and metastasis. Am J Transl Res 10: 3493-3503, 2018.
38. Andrejeva D, Kugler JM, Nguyen HT, Malmendal A, Holm ML, Toft BG, Loya AC and Cohen SM: Metabolic control of PPAR activity by aldehyde dehydrogenase regulates invasive cell behavior and predicts survival in hepatocellular and renal clear cell carcinoma. BMC Cancer 18: 1180, 2018.
39. Chen SZ, Ling Y, Yu LX, Song YT, Chen XF, Cao QQ, Yu H, Chen C, Tang JJ, Fan ZC, *et al*: 4-Phenylbutyric acid promotes hepatocellular carcinoma via initiating cancer stem cells through activation of PPAR-α. Clin Transl Med 11: e379, 2021.
40. Wagner N and Wagner KD: PPAR beta/delta and the hallmarks of cancer. Cells 9: 1133, 2020.
41. Chi T, Wang M, Wang X, Yang K, Xie F, Liao Z and Wei P: PPAR-γ modulators as current and potential cancer treatments. Front Oncol 11: 737776, 2021.
42. Livak KJ and Schmittgen TD: Analysis of relative gene expression data using real-time quantitative PCR and the 2(-Delta Delta C(T)) method. Methods 25: 402-408, 2001.
43. Li X and Meng Y: Analyses of metastasis-associated genes in IDH wild-type glioma. BMC Cancer 20: 1114, 2020.
44. Yang K, Wu Z, Zhang H, Zhang N, Wu W, Wang Z, Dai Z, Zhang X, Zhang L, Peng Y, *et al*: Glioma targeted therapy: Insight into future of molecular approaches. Mol Cancer 21: 39, 2022.
45. Christofides A, Konstantinidou E, Jani C and Boussiotis VA: The role of peroxisome proliferator-activated receptors (PPAR) in immune responses. Metabolism 114: 154338, 2021.
46. Xi Y, Zhang Y, Zhu S, Luo Y, Xu P and Huang Z: PPAR-mediated toxicology and applied pharmacology. Cells 9: 352, 2020.
47. Jimenez R, Toral M, Gómez-Guzmán M, Romero M, Sanchez M, Mahmoud AM and Duarte J: The role of Nrf2 signaling in PPARβ/δ-mediated vascular protection against hyperglycemia-induced oxidative stress. Oxid Med Cell Longev 2018: 5852706, 2018.
48. Botta M, Audano M, Sahebkar A, Sirtori CR, Mitro N and Ruscica M: PPAR agonists and metabolic syndrome: An established role? Int J Mol Sci 19: 1197, 2018.
49. Cheng HS, Tan WR, Low ZS, Marvalim C, Lee JYH and Tan NS: Exploration and development of PPAR modulators in health and disease: An update of clinical evidence. Int J Mol Sci 20: 5055, 2019.
50. Heudobler D, Rechenmacher M, Lüke F, Vogelhuber M, Pukrop T, Herr W, Ghibelli L, Gerner C and Reichle A: Peroxisome proliferator-activated receptors (PPAR)γ agonists as master modulators of tumor tissue. Int J Mol Sci 19: 3540, 2018.
51. Wang W, Wang R, Zhang Z, Li D and Yut Y: Enhanced PPAR-gamma expression may correlate with the development of Barrett's esophagus and esophageal adenocarcinoma. Oncol Res 19: 141-147, 2011.
52. Feige JN, Gelman L, Michalik L, Desvergne B and Wahli W: From molecular action to physiological outputs: Peroxisome proliferator-activated receptors are nuclear receptors at the crossroads of key cellular functions. Prog Lipid Res 45: 120-159, 2006.
53. Braissant O, Foufelle F, Scotto C, Dauça M and Wahli W: Differential expression of peroxisome proliferator-activated receptors (PPARs): Tissue distribution of PPAR-alpha, -beta, and -gamma in the adult rat. Endocrinology 137: 354-366, 1996.
54. Peters JM, Lee SS, Li W, Ward JM, Gavrilova O, Everett C, Reitman ML, Hudson LD and Gonzalez FJ: Growth, adipose, brain, and skin alterations resulting from targeted disruption of the mouse peroxisome proliferator-activated receptor beta(delta). Mol Cell Biol 20: 5119-5128, 2000.
55. Bhullar KS and Rupasinghe HP: Polyphenols: Multipotent therapeutic agents in neurodegenerative diseases. Oxid Med Cell Longev 2013: 891748, 2013.
56. Altinoz MA, Elmaci I, Hacimuftuoglu A, Ozpinar A, Hacker E and Ozpinar A: PPARδ and its ligand erucic acid may act anti-tumoral, neuroprotective, and myelin protective in neuroblastoma, glioblastoma, and Parkinson's disease. Mol Aspects Med 78: 100871, 2021.
57. Altinoz MA, Bilir A and Elmaci I: Erucic acid, a component of Lorenzo's oil and PPAR-δ ligand modifies C6 glioma growth and toxicity of doxorubicin. Experimental data and a comprehensive literature analysis. Chem Biol Interact 294: 107-117, 2018.
58. Leisewitz AV, Urrutia CR, Martinez GR, Loyola G and Bronfman M: A PPARs cross-talk concertedly commits C6 glioma cells to oligodendrocytes and induces enzymes involved in myelin synthesis. J Cell Physiol 217: 367-376, 2008.
59. Seufert S, Coras R, Tränkle C, Zlotos DP, Blümcke I, Tatenhorst L, Heneka MT and Hahnen E: PPAR gamma activators: Off-target against glioma cell migration and brain invasion. PPAR Res 2008: 513943, 2008.
60. Khoo NKH, Hebbar S, Zhao W, Moore SA, Domann FE and Robbins ME: Differential activation of catalase expression and activity by PPAR agonists: Implications for astrocyte protection in anti-glioma therapy. Redox Biol 1: 70-79, 2013.
61. Wang X, Wang G, Shi Y, Sun L, Gorczynski R, Li YJ, Xu Z and Spaner DE: PPAR-delta promotes survival of breast cancer cells in harsh metabolic conditions. Oncogenesis 5: e232, 2016.
62. Zhang J, Yang W, Zhao D, Han Y, Liu B, Zhao H, Wang H, Zhang Q and Xu G: Correlation between TSP-1, TGF-β and PPAR-γ expression levels and glioma microvascular density. Oncol Lett 7: 95-100, 2014.
63. Kolacsek O, Wachtl G, Fóthi Á, Schamberger A, Sándor S, Pergel E, Varga N, Raskó T, Izsvák Z, Apáti Á and Orbán TI: Functional indications for transposase domestications-characterization of the human piggyBac transposase derived (PGBD) activities. Gene 834: 146609, 2022.